International Journal of Mechanical, Industrial and Aerospace Sciences
ISSN: 2517-9950
Vol:9, No:1, 2015

Modelling of Heating and Evaporation of Biodiesel Fuel Droplets

Mansour Al Qubeissi, Sergei S. Sazhin, Cyril Crua, Morgan R. Heikal

***Abstract*—**This paper presents the application of the Discrete Component Model for heating and evaporation to multi-component biodiesel fuel droplets in direct injection internal combustion engines. This model takes into account the effects of temperature gradient, recirculation and species diffusion inside droplets. A distinctive feature of the model used in the analysis is that it is based on the analytical solutions to the temperature and species diffusion equations inside the droplets. Nineteen types of biodiesel fuels are considered. It is shown that a simplistic model, based on the approximation of biodiesel fuel by a single component or ignoring the diffusion of components of biodiesel fuel, leads to noticeable errors in predicted droplet evaporation time and time evolution of droplet surface temperature and radius.

***Keywords*—**Heat/Mass Transfer, Biodiesel, Multi-component Fuel, Droplet, Evaporation.

I. Introduction

BIODIESEL fuel droplets heating and evaporation are crucial processes leading to fuel combustion in the internal combustion engines [1]. As such, the accuracy of modelling these processes is important for improving the design of these engines [1]–[3]. There have been several suggestions for accurate modelling of fuel droplet heating and evaporation (see [2], [4]–[10]).

This paper presents a comparison between the results, referring to fuel droplet evaporation times and time evolution of droplet surface temperatures and radii, predicted by the previously suggested simplified models (see [11], [12]) and the recently developed version of the Discrete Component (DC) model ([9], [13], [10]). The latter takes into account the recirculation, temperature gradient, and diffusion of species inside the droplets, based on the Effective Thermal Conductivity and Effective Diffusivity (ETC/ED) models. This approach is performed in contrast with the previously suggested models that ignore temperature gradients and diffusion of species by assuming Infinite Thermal Conductivity and Infinitely fast Diffusivity (ITC/ID) of species inside the droplets.

The model originally described in [9], [13], [14] is used in the analysis. However, this model is applied to a considerably larger number of biodiesel fuels (19 types). These are: Tallow Methyl Ester (TME), Lard Methyl Ester (LME), Butter Methyl Ester (BME), Coconut Methyl Ester (CME), Palm Kernel Methyl Ester (PMK), Palm Methyl Ester (PME), Safflower Methyl Ester (SFE), Peanut Methyl Ester (PTE), Cottonseed Methyl Ester (CSE), Corn Methyl Ester (CNE), Sunflower Methyl Ester (SNE), Soybean Methyl Ester (SME), Rapeseed Methyl Ester (RME), Linseed Methyl Ester (LNE), Tung Methyl Ester (TGE), Hemp-oil Methyl Ester, produced from Hemp seed oil in Ukraine (HME1), Hemp-oil Methyl Ester, produced in European Union (HME2), Canola seed methyl ester (CAN) and Waste cooking-oil Methyl Ester (WME). The molar fractions of the pure fatty acids contributing in these methyl esters are inferred from averaging data reported in [14]–[20]. These are shown in Table I. The thermodynamic and transport properties, inferred from [9], [15], are used in the analysis.

Al Qubeissi is with the Centre for Automotive Engineering (CAE), School of Computing, Engineering and Mathematics (CEM), University of Brighton (UoB), Brighton BN2 4GJ, UK (e-mail: m.alqubeissi@brighton.ac.uk).

S.S. Sazhin is with the CAE, CEM, UoB, Brighton BN2 4GJ, UK (corresponding author, Tel: 0044 (0)1273 642677; e-mail: S.Sazhin@brighton.ac.uk).

C. Crua and M.R. Heikal are with the CAE, CEM, UoB, Brighton BN2 4GJ, UK (e-mail: C.Crua@brighton.ac.uk, M.R.Heikal@brighton.ac.uk).

II. Results and Discussion

The time evolutions of droplet surface temperatures (T_s) and radii (R_d) for the abovementioned 19 types of biodiesel fuels have been studied. It is assumed that droplets with initial temperatures and radii 350 K and 12.66 μm, respectively, are moving through air at U_d= 35 m/s at temperature and pressure equal to 880 K and 30 bar respectively.

Two examples of the time evolutions of droplet surface temperatures and radii of Rapeseed Methyl Ester (RME) and Waste oil Methyl Ester (WME) droplets are shown in Figs. 1 and 2. The following models are used in our analysis: 1) the ETC/ED model taking into account the contributions of multiple components (ME); 2) a combination of ITC and single-component models, in which all species are treated as one-component (SI); and 3) a combination of ITC and one dominant component models, in which biodiesel fuel is approximated by a single dominant component (DI). As mentioned in Section I, the second and third models are commonly used in the analysis of heating and evaporation of biodiesel fuel droplets.

TABLE I
TYPES OF BIODIESEL FUELS AND THEIR COMPOSITIONS (MOLAR FRACTIONS OF FATTY ACIDS)

Methyl Esters	Abbreviations	Fatty Acids																	
		C8:0	C10:0	C12:0	C14:0	C16:0	C17:0	C18:0	C20:0	C22:0	C24:0	C16:1	C18:1	C20:1	C22:1	C24:1	C18:2	C18:3	Others
Tallow	TME	0	0	0.20	2.50	27.90	0	23.00	0.40	0.40	0	2.50	40.00	0.30	0.30	0	2.00	0	0.50
Lard	LME	0	0	0	1.00	26.00	0	14.00	0	0	0	2.80	44.00	2.00	2.00	0	8.00	0	0.20
Butter	BME	5.19	2.80	3.40	10.99	31.66	0	10.79	0.40	0.40	0	2.40	26.37	1.00	1.00	0	3.00	0.60	0
Coconut	CME	6.00	8.00	50.00	15.00	9.00	0	3.00	0	0	0	0	7.00	0	0	0	2.00	0	0
Palm Kernel	PMK	2.60	4.00	50.00	17.00	8.00	0	1.70	1.50	1.50	0	0.40	12.00	0	0	0	1.30	0	0
Palm	PME	0	0	0.26	1.29	45.13	0	4.47	0.35	0.17	0	0.21	38.39	0	0	0	9.16	0.19	0.38
Safflower	SFE	0	0	0	0	5.20	0	2.20	0	0	0	0	76.38	0	0	0	16.22	0	0
Peanut	PTE	0	0	0	0.50	8.00	0	4.00	7.00	7.00	0	1.50	49.00	0	0	0	23.00	0	0
Cottonseed	CSE	0	0	0	2.00	19.00	0	2.00	0	0	0	0	31.00	2.50	2.50	0	41.00	0	0
Corn	CNE	0	0	0	1.00	9.00	0	2.50	0	0	0	1.50	40.00	1.00	1.00	0	44.00	0	0
Sunflower	SNE	0	0	0	0	5.92	0	4.15	1.38	1.38	0	0	18.46	0	0	0	68.41	0.30	0
Tung	TGE	0	0	0	0	3.64	0	2.55	0	13.14	0	0	10.10	0.81	0	0	13.75	51.64	4.37
Hemp1	HME1	0	0	0	0	6.62	0.21	2.06	0.45	0.25	0.23	0.33	11.88	0.27	0.17	0.15	56.71	20.67	0
Soybean	SME	0	0	0	0.30	10.90	0	4.40	0.40	0	0	0	24.00	0	0	0	52.80	7.20	0
Linseed	LNE	0	0	0	0.20	6.20	0	0.60	0	0	0	0	18.00	0	0	0	16.00	59.00	0
Hemp2	HME2	0	0	0	0	6.51	0	2.46	0.90	0	0	0	11.88	0.90	0	0	54.82	20.07	2.46
Canola seed	CAN	0	0	0	0	4.48	0.14	1.99	0.62	0.35	0.16	0.36	59.66	1.49	0.42	0	20.89	9.44	0
Waste oil	WME	0	0	0.20	0.67	15.69	0.20	6.14	0.39	0.44	0.30	0.73	42.84	0.56	0.15	0	29.36	2.03	0.30
Rapeseed	RME	0	0	0	0	4.93	0	1.66	0.56	0	0	0	26.61	0	22.32	0.77	24.75	9.70	8.70

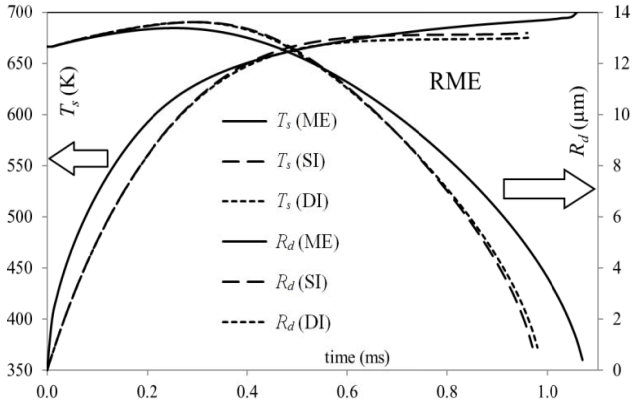

Fig. 1 The droplet surface temperature (T_s) and radius (R_d) versus time predicted by the ME, SI and DI models, for a RME fuel droplet

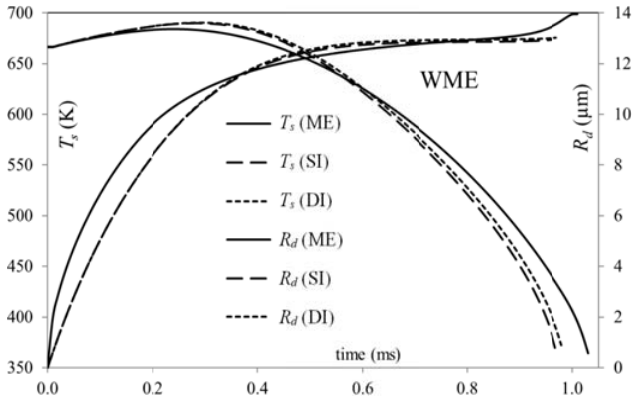

Fig. 2 The same as Fig. 1, but for a WME fuel droplet

As one can see from Figs. 1 and 2, the errors in predictions of the droplet surface temperatures, radii and evaporation time using the conventional (single-component SI or dominant-component DI) models, compared with the predictions of the ME model, are noticeable and should not be ignored in practical engineering applications. The deviations between the predictions of these two models and the ME model indicate the importance of taking into account the diffusion of species inside droplets alongside the effects of temperature gradient in them. These errors in droplet evaporation times, predicted by the SI model compared to the ME model, have been estimated for RME and WME to be up to 9.4% and 5.9%, respectively. Also, the errors in droplet surface temperatures, predicted by the SI model compared to the ME model, for RME and WME have been shown to be up to 10.6% and 10.5%, respectively.

These errors in evaporation times and temperatures are similar to those inferred from the application of the DI model compared to ME model for both types of biodiesel fuels (see Figs. 1 and 2). The trends of the plots shown in Figs. 1 and 2 are reasonably close to the ones reported in [9], [12], [14]. The errors in evaporation times and temperatures, predicted by the SI and DI models are related to the fact that diffusion of species in the droplets are not taken into account in these models.

The plots of surface mass fractions of selected species versus time for RME and WME, predicted by the ME model, are shown in Figs. 3 and 4 respectively.

As one can see from Figs. 3 and 4, the heaviest components become the dominant ones at the late stage of evaporation (e.g. C24:1 M, for RME, and C24:0 M, for WME), even when their contributions at the initial stage are very small. At the same time, the lightest components become the least contributing ones at the late stages of evaporation, even when their initial contributions are relatively large (e.g. C16:0M, C18:2 and C18:3, for RME, and C16:0M, for WME). The molar fractions of intermediate components initially increase

with time, but later their contributions decrease and near the end of evaporation time these contributions become negligible.

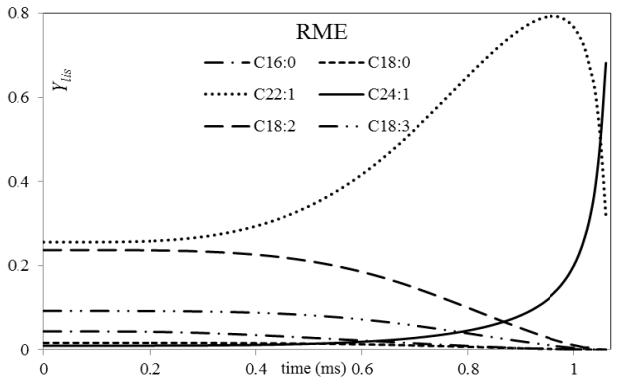

Fig. 3 The plots of time evolution of surface mass fractions of C16:0M, C18:0M, C22:1M, C24:1M, C18:2M and C18:3M for a RME droplet under the same conditions as in Figs. 1 and 2

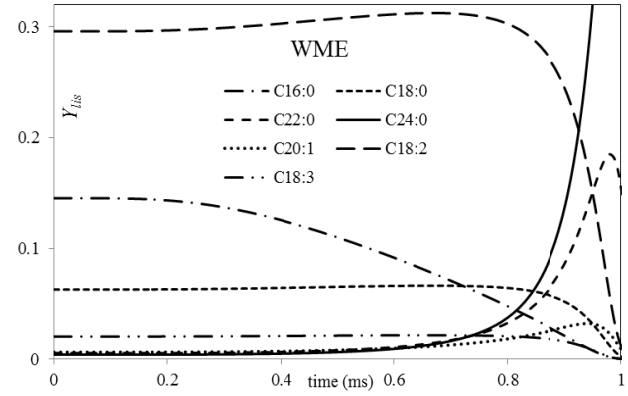

Fig. 4 The plots of time evolution of surface mass fractions of C16:0M, C18:0M, C22:0M, C24:0M, C20:1M, C18:2M and C18:3M for a WME droplet under the same conditions as in Figs. 1-3

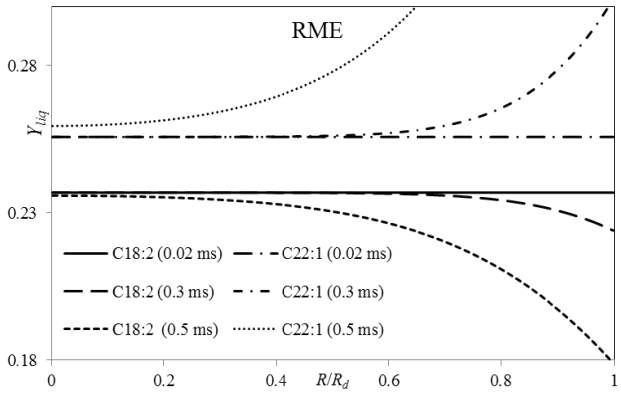

Fig. 5 The plots of mass fractions of C18:2M and C22:1M versus normalised distance from the centre of the droplet at three time instants 0.02 ms, 0.3 ms and 0.5 ms for a RME droplet under the same conditions as in Figs. 1-4

The plots of mass fractions of selected components versus normalised distance from the droplet centre at various time instants, for RME and WME, are shown in Figs. 5 and 6, respectively.

In agreement with the results shown in Figs. 3 and 4, one can see from Figs. 5 and 6 that the lighter components (e.g. C18:2M, for RME, and C12:0M, for WME) evaporate quicker than the heavier components (e.g. C22:1M), which leads to decrease in mass fractions of the lighter components in the vicinity of the surface of the droplet. Also, it can be seen from these figures that the gradients of species mass fractions formed inside droplets increase with time.

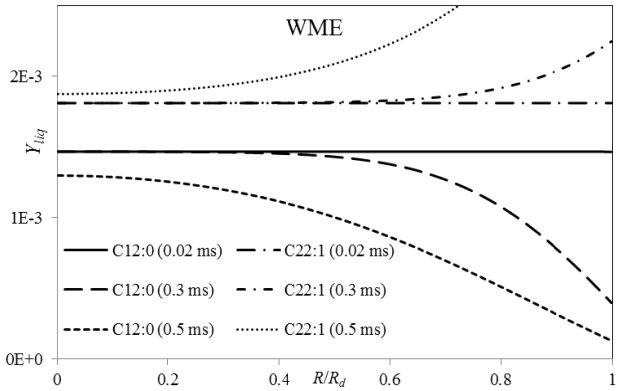

Fig. 6 The plots of mass fractions of C12:0M and C22:1M versus normalised distance from the centre of the droplet at three time instants 0.02 ms, 0.3 ms and 0.5 ms for a WME droplet under the same conditions as in Figs. 1-5.

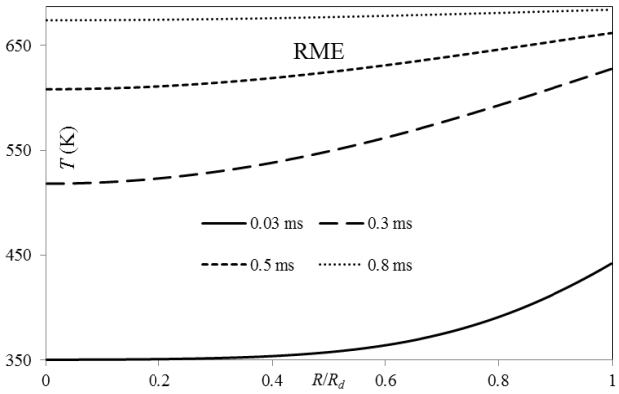

Fig. 7 The plots of temperature versus normalised distance from the centre of droplet at four time instants 0.03 ms, 0.3 ms, 0.5 ms and 0.8 ms for a RME droplet under the same conditions as in Figs. 1-6

The plots of temperatures inside the droplet of RME and WME biodiesel fuel droplets versus normalised distance from the centre of the droplet at four time instants (0.03 ms, 0.3 ms, 0.5 ms and 0.8 ms) are shown in Figs. 7 and 8, respectively.

As one can see in Figs. 7 and 8, at the initial stage of droplet heating and evaporation (0.03 ms after the start of the process) a rather large gradient of temperature inside the droplet close to droplet surface is formed. In contrast to the case of species

mass fractions, however, the gradients of temperature inside droplets decrease with time. These gradients are reasonably small at 0.8 ms after the start of the process. This means that the Infinite Thermal Conductivity model can be applied to the analysis of droplet heating and evaporation, except at the very beginning of the process, when high accuracy of calculations is not required.

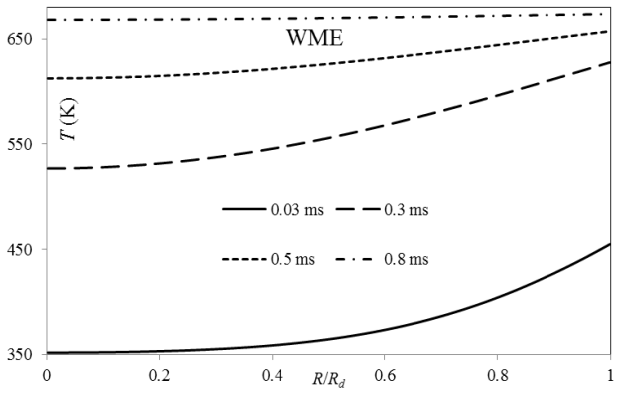

Fig. 8 The plots of temperature versus normalised distance from the centre of droplet at four time instants 0.03 ms, 0.3 ms, 0.5 ms and 0.8 ms for a WME droplet under the same conditions as in Figs. 1-7

III. Conclusion

Ignoring the effects of species diffusion, temperature gradient and recirculation inside droplets, or assuming that these species can be replaced by a single-dominant component, which are common practices in modelling heating and evaporation of biodiesel fuel droplets in many engineering applications, can lead to noticeable errors in the predictions of droplet surface temperatures and evaporation times. It is recommended that the Effective Thermal Conductivity/Effective Diffusivity (ETC/ED) model, taking into account diffusion of all species, is used for the analysis of these processes.

Acknowledgments

The authors are grateful to Mr Jack Turner for useful discussions and to INTERREG IVa (Project E3C3, Reference 4274) and University of Brighton for their financial support to the project.

References

[1] S. S. Sazhin, *Droplets and Sprays*. London: Springer-Verlag, 2014.
[2] B. Abramzon and S. S. Sazhin, 'Convective vaporization of a fuel droplet with thermal radiation absorption', *Fuel*, vol. 85, no. 1, pp. 32–46, Jan. 2006.
[3] W. A. Sirignano, *Fluid Dynamics and Transport of Droplets and Sprays*. Cambridge, U.K: Cambridge University Press, 1999.
[4] B. Abramzon and S. Sazhin, 'Droplet vaporization model in the presence of thermal radiation', *Int. J. Heat Mass Transf.*, vol. 48, no. 9, pp. 1868–1873, Apr. 2005.
[5] A. E. Elwardany and S. S. Sazhin, 'A quasi-discrete model for droplet heating and evaporation: Application to Diesel and gasoline fuels', *Fuel*, vol. 97, pp. 685–694, Jul. 2012.
[6] A. E. Elwardany, S. S. Sazhin, and A. Farooq, 'Modelling of heating and evaporation of gasoline fuel droplets: A comparative analysis of approximations', *Fuel*, vol. 111, pp. 643–647, Sep. 2013.
[7] A. E. Elwardany, I. G. Gusev, G. Castanet, F. Lemoine, and S. S. Sazhin, 'Mono- and multi-component droplet cooling/heating and evaporation: comparative analysis of numerical models', *At. Sprays*, vol. 21, no. 11, pp. 907–931, 2011.
[8] S. S. Sazhin, 'Advanced models of fuel droplet heating and evaporation', *Prog. Energy Combust. Sci.*, vol. 32, no. 2, pp. 162–214, 2006.
[9] S. S. Sazhin, M. Al Qubeissi, R. Kolodnytska, A. E. Elwardany, R. Nasiri, and M. R. Heikal, 'Modelling of biodiesel fuel droplet heating and evaporation', *Fuel*, vol. 115, pp. 559–572, Jan. 2014.
[10] M. Al Qubeissi, S. S. Sazhin, G. de Sercey, and C. Crua, 'Multi-dimensional quasi-discrete model for the investigation of heating and evaporation of Diesel fuel droplets', in *26th European Conference on Liquid Atomization and Spray Systems*, Bremen, Germany, 2014.
[11] S. S. Sazhin, A. Elwardany, P. A. Krutitskii, G. Castanet, F. Lemoine, E. M. Sazhina, and M. R. Heikal, 'A simplified model for bi-component droplet heating and evaporation', *Int. J. Heat Mass Transf.*, vol. 53, no. 21–22, pp. 4495–4505, Oct. 2010.
[12] S. Tonini and G. E. Cossali, 'A novel vaporisation model for a single-component drop in high temperature air streams', *Int. J. Therm. Sci.*, vol. 75, pp. 194–203, Jan. 2014.
[13] M. Al Qubeissi, R. Kolodnytska, and S. S. Sazhin, 'Biodiesel fuel droplet: modelling of heating and evaporation processes', in *25th European Conference on Liquid Atomization and Spray Systems*, Crete, Greece, 2013.
[14] S. S. Sazhin, M. Al Qubeissi, and M. R. Heikal, 'Modelling of biodiesel and diesel fuel droplet heating and evaporation', in *15th International Heat Transfer Conference, IHTC-15*, Kyoto, Japan, 2014, vol. IHTC15–8936.
[15] R. Kolodnytska, M. Al Qubeissi, and S. S. Sazhin, 'Biodiesel fuel droplets: transport and thermodynamic properties', in *25th European Conference on Liquid Atomization and Spray Systems*, Crete, Greece, 2013.
[16] T. M. Mata, N. Cardoso, M. Ornelas, S. Neves, and N. S. Caetano, 'sustainable production of biodiesel from tallow, lard and poultry fat and its quality evaluation', in *Chemical engineering transactions*, 2010, vol. 19.
[17] S. Dirbude, V. Eswaran, and A. Kushari, 'Droplet vaporization modeling of rapeseed and sunflower methyl esters', *Fuel*, vol. 92, no. 1, pp. 171–179, Feb. 2012.
[18] K. S. Tyson, J. Bozell, R. Wallace, E. Petersen, and L. Moens, 'Biomass Oil Analysis: Research Needs and Recommendations', National Renewable Energy Lab., Golden, CO (US), NREL/TP-510-34796, Jun. 2004.
[19] J.-Y. Park, D.-K. Kim, Z.-M. Wang, P. Lu, S.-C. Park, and J.-S. Lee, 'Production and characterization of biodiesel from tung oil', *Appl. Biochem. Biotechnol.*, vol. 148, no. 1–3, pp. 109–117, Mar. 2008.
[20] E. G. Giakoumis, 'A statistical investigation of biodiesel physical and chemical properties, and their correlation with the degree of unsaturation', *Renew. Energy*, vol. 50, pp. 858–878, Feb. 2013.